Q. J. R. Meteorol. Soc. (1992), **118**, pp. 101–124 551.515.41:551.515.81

The development of organized convection in a simplified squall-line model

By S. T. GARNER[1] and A. J. THORPE
Department of Meteorology, University of Reading

(Received 12 October 1990; revised 1 May 1991)

SUMMARY

Squall lines stand out from ordinary cumulonimbus convection because of a special structure that dramatically extends their duration, precipitation output and area of influence. Time-dependent models have identified surface outflow boundaries and low-level environmental wind shear as the crucial elements in squall-line formation and/or maintenance. Steady-state models have shown how properties of the downdraught reservoir, or 'cold pool', must be matched to the far-field wind and thermodynamic profiles to sustain the convection. However, the dynamical role of the environmental shear and the nature of the interaction between the positively and negatively buoyant air have remained uncertain. For help with these issues, a time-dependent numerical model is developed with all moist processes either parametrized or based on *ad hoc* assumptions. The simplifications make it possible to distinguish more clearly than in the past between the formation and maintenance of squall lines and between the initial and disturbed far-field environments.

The convective updraught forms within an expanding region of disturbed flow separated from the undisturbed environment by 'storm fronts'. Forced (or neutral) ascent occurs at a surface 'gust front' on the upwind side of the cold pool. We distinguish squall lines from ordinary convection by looking at the coherence between the forced and convective updraughts. It is found that subsidence over the cold pool disorganizes the updraughts, whereas a deep overturning circulation downshear from the gust front has an organizing effect. Hence, factors which allow the initial subsidence to occur ahead of the gust front, namely contrasting lower- and upper-level winds and large potential buoyancy, favour squall-line development. It is argued that, in cases with large convective potential energy, the deep mesoscale circulation is more important in the formation and maintenance of the line than either the vertical shear of the air reaching the cold pool or the strength of the forced updraught.

1. INTRODUCTION

Moist convection can become organized into a squall line if a component of the environmental wind (the component normal to the line) has its vertical shear concentrated in low levels and if conditions favour the formation and maintenance of a strong surface cold pool. Indeed, observations and simulations show that line convection under these conditions can be sustained without forcing from orography, synoptic-scale fronts or internal waves. Physical improvements in models of moist convection have not necessarily made it easier to understand how the shear and cold pool help to develop a sustainable mesoscale structure. Our aim here is to use a physically simple, two-dimensional numerical model to highlight this development.

The proposed model resolves finite-amplitude, non-hydrostatic convective updraughts and downdraughts, but a significant simplification is achieved by parametrizing fully the effects of condensation and evaporation (so that moisture does not appear as an explicit variable). This eliminates microphysical and precipitation time-scales and makes it easier to distinguish the development of squall lines from their quasi-steady state. Certain theories about the significance of the shear can then be tested more readily. It will be seen that the simple treatment of moisture does not prevent the development of quasi-steady temperature and flow structures similar to those in more sophisticated two-dimensional models. The early phase of the simulations also shows many realistic features.

According to a conceptual model derived from full-cloud-model simulations (Thorpe *et al.* 1982), the role of the shear in squall lines is to provide a low-level storm-relative wind to restrain the cold pool. It is equivalent to say that the upper-level wind 'carries'

[1] Current affiliation: GFDL, Princetown University, New Jersey 08542

the convective updraught at the speed of the gust front (the edge of the spreading cold pool). However, no plausible way in which the updraught can actually acquire the upper-level flow speed has ever been spelled out. Nonlinear analytical models (e.g., Moncrieff and Miller 1976; Moncrieff and So 1989) also fall short of identifying the role of the shear, not only because they consider the squall line in isolation from the undisturbed environment (except for inflow thermodynamic conditions), but also because they *impose* a coherence between the updraught and density current through an assumption of steadiness. The resulting necessary conditions on the far-field wind and temperature profiles do not ensure the possibility of a steady internal structure.

The spatial relationship between the gust front and buoyant updraught determines the total updraught tilt. Browning and Ludlam (1962) and Emanuel (1986) have emphasized that some upshear tilt is required in order to decouple condensation from evaporation. However, it is clear that an extreme tilt can effectively stanch the supply of potentially buoyant surface air to the convection. This can be avoided if new cells develop soon after the old ones begin to weaken; indeed, a number of recent numerical studies (Dudhia *et al.* 1987; Redelsperger and Lafore 1988; Rotunno *et al.* 1988; Fovell and Ogura 1988) have emphasized that the buoyancy decoupling can be accomplished partly in the time dimension, through quasi-periodic cell decay and redevelopment. Redevelopment can also be seen in the simulations by Thorpe *et al.* (1982). Thus, in models with sophisticated microphysical parametrizations, there may not be any strict coherence between the gust front and the core of free convection.

In its early phase, the simulation by Rotunno *et al.* (1988, hereafter RKW) shows an essentially vertical updraught (on average over time), so that the aforementioned decoupling depends almost entirely on temporal alternation between updraught and downdraught. Based on these results, RKW have challenged the view that the cold pool must be 'restrained' to match the motion of the convection. They suggest that the convection is so strongly modulated by the gust front that the speed of the cold pool *with respect to the upper-level flow* is not directly important. The squall line is identified as the succession of cumulonimbus lifecycles, which are seen as disturbing the larger environment only to the extent of generating and regenerating quasi-two-dimensional outflow boundaries at the ground. Hence, RKW argue that the strength and longevity of the convective ensemble depend mainly on details of the forced updraughts at the surface. In particular, environmental shear must be present to 'counteract' the vorticity of the gust front and yield an 'optimal' (i.e. vertical) forced updraught (for convenience, 'forced updraught' is used to include both negatively and neutrally buoyant ascent).

The view of RKW minimizes the distinction between the development and maintenance of a squall line. At odds with this view is the recent study of tropical squall lines by Lafore and Moncrieff (1989), who play down the role of the cold pool in directly modifying the surface inflow to the updraught. Instead, they emphasize the disturbed nature of the inflow and outflow circulations. We are especially interested in modelling these larger circulations, whose 'spin-up' represents most of the transience at scales somewhat bigger (and longer) than an individual cell. After their development and that of the cold pool, the kind of variability on which RKW's theory is based cannot be seen as occurring in an undisturbed environment. Thus, Moncrieff (1978) refers to the embedded cells as 'superposed transience'. The proposed model naturally highlights the development of the inflow/outflow circulations and cold pool.

The possibility, in nature, of a steady upshear-tilted updraught is not entirely ruled out. New Doppler radar observations presented by Meischner *et al.* (1991) show that the permanent part of the main updraught strongly dominates the transient smaller updraughts embedded within it. Highly steady structures, or superlines, would be the two-dimensional counterparts of supercells. Although they may be exceptional among long-lived convective systems, it would be surprising if a theory of superlines had no application to squall lines whose vertical mass flux is dominated by transient cumulonimbus cells. In such cases, the upshear tilt is generally quite apparent in the *time-averaged* circulation, from which the relative movement of the dying cells and surging cold pool has been filtered.

In eliminating the main cause of cell decay, i.e. explicit downdraughts of rain-cooled and rain-loaded air, the proposed model assumes that the effect of buoyancy fluxes produced by the cell-related variability can be parametrized realistically from the resolved motion. The effect of the dense downdraughts is thus reduced to the effect of the cold pool, and the net latent heating is made strictly coincident with model updraughts. To interpret the results, we will assume that continual redevelopment is implicit if, and only if, the convective updraught in the model becomes quasi-steady in the frame of the gust front (the condition of spatial coherence) and is consistent with the necessary temporal and spatial decoupling between condensation and evaporation (the condition of upshear tilt). Thus, we are also investigating the conditions needed to maintain a superline.

Rotunno *et al.* (1990) have emphasized that the counteraction mechanism proposed by RKW is given as a necessary, rather than sufficient, condition for strong, long-lived squall lines. However, Lafore and Moncrieff (1990) have concluded that the condition is not closely related to the strength of the convection in tropical squall lines possessing extensive stratiform regions. They attribute the discrepancy to the importance of larger-scale features such as the tilt of the total updraught, including its mid- and upper-tropospheric parts. These are the features that we intend to investigate. With cell transience suppressed, our model cannot reveal whether RKW's condition of optimal updraughts is necessary for redevelopment. However, we will be in a position to examine the relevance of the condition to the strength of the convection.

We have not tried to parametrize the effect of momentum fluxes due to cell redevelopment or three-dimensionality, except insofar as they cause down-gradient mixing. Otherwise, their effect on the resolved updraught tilt, for example, is missing. This neglect is justified by some results of Fovell and Ogura (1988), who found that the eddy contribution to the horizontal momentum budget in a two-dimensional simulation is much smaller—by a factor of about 5 (their Fig. 12)—than the contribution from the time-mean circulation. The appropriateness of simplifying to two dimensions has been discussed by Moncrieff (1978) and others. With the theoretical exception of non-interactive groupings of supercells (Lilly 1979), the organization of long-lived convection does not seem possible without continuous, quasi-two-dimensional inflow and outflow perturbations at the top and bottom of the troposphere. Stronger justification for assuming slab symmetry has been provided by RKW, who carried out comparable two- and three-dimensional numerical simulations. They concluded that 'the essential physics of this type of squall line is contained in the two-dimensional framework.'

The present approach does not consider whether the cold pool is necessary for organizing and maintaining squall lines. Thus, alternative propagation mechanisms such as internal gravity waves and 'wave-CISK' (Raymond 1983) are not examined. Wave-CISK (Conditional Instability of the Second Kind) describes amplifying, linearized convection and has not been demonstrated (to our knowledge) in a convection-resolving numerical simulation. Nevertheless, certain qualitative similarities will be pointed out between the propagation of parametrized convection as deduced from linear theory and the development of explicit convection as deduced from the present finite-amplitude simulations.

2. A SIMPLIFIED NUMERICAL MODEL OF SQUALL LINES

The explicit representation of moisture in cloud models can make it difficult to judge the importance of different competing and co-operating effects, and steady-state analytical models avoid the question of development altogether. The model to be described here is capable of representing long-lived structures in considerable detail and showing how they arise from initial conditions. However, as stated in the introduction, transience is suppressed by fully parametrizing the effects of latent heat and precipitation drag on the buoyancy. Whenever moist processes are parametrized, it is of course necessary to pay close attention to the physical consistency of the solutions.

As in most previous work, we neglect the earth's rotation and any explicit three-dimensional effects. Compressible and non-Boussinesq effects are also neglected, and rigid upper and lower boundaries are assumed. The only sophistication of the numerical model is the use of a flux-corrected transport scheme (Zalesak 1979) to advect potential temperature. This cuts down on implicit mixing and thus gives greater control over the introduction of negative buoyancy into the updraught. With moisture fully parametrized, the only other prognostic variable is the horizontal vorticity, which uniquely determines the flow under the foregoing assumptions. Vorticity is used as a model variable instead of pressure because it is conserved except for readily understood sources and sinks.

The vorticity and stream function are defined at grid points staggered in both directions from potential-temperature points. The prognostic vorticity equation is evaluated in flux form using a second-order accurate (anti-diffusive) upstream advection scheme. Open lateral boundaries are approximated with a wave-advection lateral boundary condition (Orlanski 1976) on both the vorticity and the temperature. Despite its name, this condition works well on nonlinear disturbances if structures remain coherent as they approach the boundary. By varying the domain size, it was ascertained that this way of handling the computational boundaries eliminates any significant influence from them.

(a) *Thermodynamics of the model*

Moist processes generate buoyancy of either sign, depending on the direction of the phase change. Letting b denote the potential buoyancy for the Boussinesq model (see appendix for definitions of variables), we write $\mathrm{d}b/\mathrm{d}t = Q_+ + Q_-$, where Q_+ and Q_- represent separate non-adiabatic heating and cooling processes, respectively. The condensational heating is made conditionally proportional to the vertical velocity, w, according to:

$$Q_+ = \begin{cases} \gamma w, & w > 0 \\ 0, & w \leq 0 \end{cases} \qquad (1)$$

where γ is a specified, non-negative function of height, z. The diagram in Fig. 1 illustrates the choice for $\gamma(z)$ by showing the variation with height of the potential temperature of a parcel of air lifted from the ground to the upper boundary. Note that γ is a positive constant from $z = h_\mathrm{b}$ (cloud base) to a higher level $z = h_\mathrm{m}$, and zero above and below. The layer below h_b is intended to approximate a well-mixed unsaturated boundary layer, while the uppermost layer corresponds to the 'dry' part of a moist adiabat. The uniform height of the cloud base implies that the specific humidity is also well mixed in the surface layer.

As shown in Fig. 1, the initial potential-temperature profile $\bar{b}(z)$ is linear in three sections, with changes in stratification occurring at $z = h_\mathrm{b}$ and $z = h_\mathrm{m}$. The layer below $z = h_\mathrm{b}$ is taken to be neutrally stratified. The change to stronger stratification at the higher level allows ascending air to reach neutral buoyancy (relative to the undisturbed

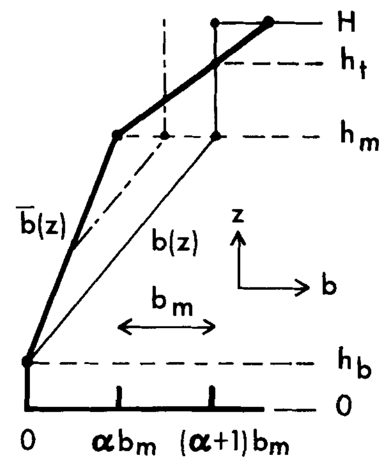

Figure 1. Thermodynamic profiles showing initial potential temperature, $\bar{b}$, (heavy solid line) and potential temperature of lifted parcels (thin solid and dot-dashed). Thin lines to the right of the initial profile indicate buoyant parcels. Those to the left indicate overshooting past the level of neutral buoyancy. See text for explanation of symbols.

environment) somewhere between the level of maximum buoyancy at $z = h_m$ and the upper boundary at $z = H$. The highest possible level of neutral buoyancy is denoted h_t and applies to parcels originating at or below $z = h_b$; parcels originating from above cloud base reach neutral buoyancy somewhat lower, as illustrated by the dot-dashed line. The initial potential temperature at $z = h_m$ is expressed as $\bar{b} = \alpha b_m$, where b_m is the maximum relative buoyancy of lifted parcels.

It is known from field measurements of equivalent potential temperature (e.g. Ogura and Liou 1980; Smull and Houze 1985) and from simulations of squall lines (Fovell and Ogura 1988; Lafore and Moncrieff 1989) that the cold pool is fed primarily by mid-tropospheric air in which ice has melted or rainwater has evaporated. The main dynamical effect of these phase changes and the resulting cold downdraughts will be simulated by continuously cooling a region of the domain near the ground towards a fixed minimum buoyancy, b_c, representative of the mid-tropospheric wet-bulb potential temperature. Thus, the non-adiabatic cooling is prescribed as:

$$Q_- = \begin{cases} -(b - b_c)/\tau_c, & -l_c < x < 0 \text{ and } z < h_c \\ 0, & \text{elsewhere} \end{cases} \tag{2}$$

where τ_c is a relaxation time of the order of a few minutes. This scheme differs from that of Thorpe *et al.* (1982, hereafter TMM) and other models employing cold-pool initiation because we use a target temperature and because the cooling remains active against dissipation throughout the simulation.

Because explicit downdraughts are assumed to be subsaturated in using Eq. (1), it is physically inconsistent to apply the heating as soon as $w > 0$ if the air has recirculated. To compensate for unphysical reheating in closed circulations at the edge of the developing 'anvil', a small value $\alpha = 1$ is used for forced stable descent. This value is still large enough for significant warming to occur around the updraught due to broad-scale adiabatic descent. Moist convection is quite sensitive to subsidence warming, which is inherently difficult to simulate correctly in a limited-area model, especially in two dimensions.

(*b*) *Dynamics of the model*

The horizontal vorticity, η, is changed by buoyancy gradients and diffusion according to:

$$\mathrm{d}\eta/\mathrm{d}t = -\partial b/\partial x + D_\eta \tag{3}$$

where D_η represents explicit diffusion. The velocity is recovered from the vorticity in the usual way by solving $\nabla^2\psi = \eta$ and evaluating $u = \partial\psi/\partial z$ and $w = -\partial\psi/\partial x$ for the horizontal and vertical components, respectively. There is no assumption of hydrostatic balance.

Explicit mixing is included for computational purposes by setting

$$D_\eta = K\left(\frac{\partial^2}{\partial x^2} + \delta^2\frac{\partial^2}{\partial z^2}\right)(\eta - \overline{\eta})$$

where K is a uniform eddy diffusivity coefficient for momentum and δ is a mixing-aspect ratio ($\overline{\eta}$ is the vorticity of the initial state). Neumann conditions ($\partial\eta/\partial z = 0$) are imposed at the rigid boundaries. This allows a cross-boundary eddy flux of momentum but not of vorticity. In all of the simulations we use $\delta^2 = 1/10$ and $K = (1/5)\gamma^{1/2}(H/10)^2$. For typical parameter values, this choice tends to remove features with a horizontal scale of 1 km in about 25 min. There is no explicit thermal diffusion, but a significant amount of implicit diffusion may arise from the finite-differencing of $\partial b/\partial x$.

The value of the stream function ψ is held constant in time at both boundaries. This means that the cooling region is fixed in the frame that maintains the initial vertically integrated horizontal mass flux, or:

$$M \equiv \psi(H) - \psi(0) = \int_0^H u\mathrm{d}z.$$

Since the flow is incompressible, this frame translates at a uniform speed with respect to the undisturbed environment. If steady states are possible for a given initial profile shape, they are expected to fall into a narrow range of values of M, corresponding to the possible speeds of the mature line through the undisturbed environment.

Acceptable steady states must pass a test of physical consistency based on the behaviour of the cold pool. Solutions are inconsistent if the gust front is pushed far into the cooling region or allowed to spread so far the other way as to be distinctly warmer than the imposed downdraught temperature. In these two cases, the model cooling behind the gust front is too strong or too weak, respectively, to be consistent with the updraught structure and location of the cold downdraughts implied by Eq. (2). Vertical or downshear-tilting updraughts are also unphysical, as discussed in the Introduction. The restrictions on the behaviour of the gust front do not preclude a certain amount of penetration of the cold pool by the surface inflow, which is a realistic consequence of mixing.

Although the initial wind profile is important in determining the susceptibility of the environment to squall-line organization, it is profoundly altered by the development of the deep convection. To emphasize the transformation, we show schematically in Fig. 2 the development process based on a number of simulations. The frame of reference is that of the steady state, with the initial low-level wind coming from the right. Note especially the possibility of complete flow reversal over time at the upper right and middle left. Of the initial profile characteristics, all that remain after the squall line has developed are the original net horizontal mass flux and the vorticity of any permanent (unreversed) inflow layers. For example, since there is no mechanism for changing the shear near the ground far upstream, the vorticity in most of the jump updraught feeder is permanent.

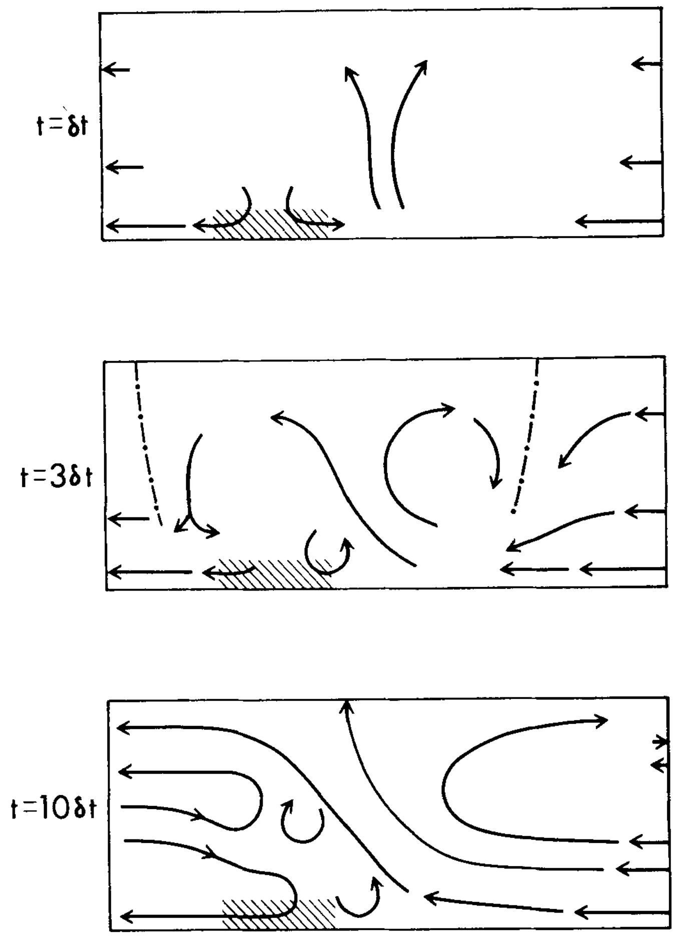

Figure 2. Schematic time sequence illustrating squall-line development. Top panel: initial 'thermal' splits to form jump and overturning updraughts; mid-level air subsides into cooling region (hatched). Middle panel: updraught produces subsidence 'waves' upshear and downshear from gust front (dot-dashed lines indicate storm fronts). Bottom panel: overturning circulations establish new surface wind at right and elevated inflow jet at left; cold rotor circulation develops behind gust front.

Subject to this constraint, the velocities in that layer are free to vary. During start-up, the cold pool undergoes frontogenesis at its downshear edge, which may drift or oscillate slightly toward its steady position.

Above the permanent surface-inflow layer, the flow is converted to an overturning updraught through *nonlinear* advection of perturbation vorticity. The vorticity is generated in the developing plume and at the leading edge of the buoyant air as it spreads out near the level of neutral buoyancy. Since the overturning updraught has no net mass flux, its presence increases the low-level horizontal mass flux by the amount of any initial mass flux it displaces. This gives rise to the aforementioned surface velocity changes and a vertical transfer of mass into the inflow layer between the squall line and undisturbed environment. An associated Bernoulli-effect pressure drop (typically of 1 or 2 mb) marks the passage of the storm front, shown as a dot-dashed line in the diagram. The incompressibility assumption (made in the spirit of maximum simplification) overestimates the displaced upper-level mass flux over a given depth. However, it seems to have little influence on the evolution of the surface flow, as we will explain in section 3.

Much of the adiabatic subsidence warming in the model is concentrated in the upper part of the storm fronts. Observations from the tropics seem to show that the temperature at upper levels adjusts to the environmental stratification behind the squall line (Betts 1976). On the contrary, two-dimensional simulations show a permanent alteration of the upper-level temperature stratification. In nature, the squall-line disturbance is bounded in both the line-parallel and line-normal directions. Hence, the restoration of pre-squall conditions is probably due to the passage of the disturbance through the observing network in either direction.

The storm fronts mark the limits of the far-field influence. Because of a traditional emphasis on steady structures, past research has overlooked this feature of cumulonimbus dynamics, including its involvement in storm development and its contribution to heat and momentum fluxes. The storm front is neglected in the analyses of Moncrieff and So (1989) and RKW, for example, which seek predictions of the gust-front speed relative to the low-level wind that develops within the disturbed region. The 'propagating' and 'cellular' models of Moncrieff (1981) both contain aspects of the storm front, but are limited by the assumption of a fixed separation between the subsiding or propagating part of the storm and the main updraught (no steady model can adequately incorporate a storm front).

Neglecting the storm front is equivalent to assuming an infinite signal speed for the far-field influence. We will argue that the very possibility of downshear influence may be crucial in squall-line formation, and that a more subtle parameter than the local gravity-current speed is the system speed relative to the undisturbed environment, i.e. the speed associated with M. The neglect of downshear influence was one of the weaknesses of the RKW theory cited by Lafore and Moncrieff (1990). We mention in the next section how M is chosen experimentally in finding quasi-steady model solutions, and suggest in section 5 how the critical value might be determined from dynamical theory.

3. Model simulations

The simplicity of the numerical model allows a thorough investigation of the sensitivity to wind profiles and other external parameters. To avoid performing essentially identical experiments, we relate all distances to H, buoyancies to b_m, time constants to $\tau_m \equiv \surd(H/b_m)$ and velocities to $V_m \equiv \surd(b_m H)$. Since b_m is proportional to the maximum lifted potential-temperature anomaly in the sounding, velocities normalized by V_m are Froude numbers based on the convective available potential energy (CAPE) per unit mass, which equals $\frac{1}{2}V_m^2(h_t - h_b)/H$. These differ from Froude numbers based on properties of the cold pool, from which the independent velocity scale $V_c = \surd(-b_c h_c)$ can be formed.

Observational studies of mid-latitude squall lines typically show a maximum lifted temperature of about 6 K (e.g. Bluestein and Jain 1985), which yields $b_m \approx 0.2\,\mathrm{m\,s^{-2}}$. However, simulated storms never produce this large an anomaly within a significant volume of air. A more realistic choice, taking into account a certain convective inefficiency not otherwise present in our *ad hoc* model, is $b_m = 0.1\,\mathrm{m\,s^{-2}}$. In that case, $V_m \approx 30\,\mathrm{m\,s^{-1}}$ if the upper boundary height is $H = 10\,\mathrm{km}$. The corresponding time-scale τ_m (a measure of the residence time of parcels in the convective updraught) is about 5 min. A realistic buoyancy for the cold pool is $b_c = -0.15\,\mathrm{m\,s^{-2}}$. The cold pool tends to be less dilute in cloud-model simulations than the warm thermals. Because $h_c \ll H$, the gravity-current velocity scale V_c is typically only about half of the convective scale V_m.

The top of the latent-heating layer (the level of maximum buoyancy) will be fixed at $h_m = 0.7H$ for all simulations, and the level of neutral buoyancy at $h_t = 0.9H$. The cloud base is put at $h_b = 0.10H$. The cooling region is given a width $l_c = 1.0H$ and a depth $h_c = 0.15H$. It is not unreasonable to have the cooling deeper than cloud base, as the cool air originates at middle levels rather than in the surface layer. The grid intervals are $\Delta z = H/33$ and $\Delta x = H/12$, with the lateral boundaries at $x = \pm 4.5H$. Hence, the horizontal resolution falls between that of RKW (2 km) and TMM (0.5 km). The vertical resolution is more than twice as fine as in those studies, so that the shallowest part of the cold pool is resolved by 3 or 4 grid points in the vertical, compared with 1 or 2 in the earlier work. A leap-frog time-stepping scheme is used, with $\Delta t = \tau_m/50$.

The initial flow at the ground is always from right to left; hence, the gust front forms on the right side of the cold pool and the jump updraught exits to the left, as in Fig. 2. The creation of the cold pool triggers the convection by producing low-level convergence and lifting. In the following, the organizational process will be studied first, with quantitative details of the steady states being deferred to the end of the section. The frame of reference in the solutions is determined by the choice of average wind speed in the environmental profile. This choice affects M without changing the shape of the profile. In investigating development criteria, M is chosen to keep the gust front near the centre of the domain (therefore near the right-hand edge of the cooling region) throughout the simulation. This means taking $M \approx M^*$, where M^* is the mass flux in the frame of the steady system (if one exists).

(*a*) *Sensitivity to low-level shear*

We concentrate first on the sensitivity to initial low-level shear and depth of the shear layer. The flow is initiated with uniform positive shear, $\bar{\eta} = \eta_0$, where $\bar{\eta} \equiv d\bar{u}/dz$, extending from the lower boundary to a height h_0, and $\bar{\eta} = 0$ from that level to the upper boundary. Such profiles have been identified by TMM as optimal for squall-line organization. For a range of choices of η_0 and h_0, the model achieves realistic quasi-steady states within roughly the first hour ($\Delta t = 12\tau_m$), while for other choices the flow fails to converge to a realistic structure over the duration of the simulation ($\Delta t = 48\tau_m$). We will show one example of each case.

In 'failed' simulations, the convection (free updraught) drifts unrealistically far upshear from the gust front (forced updraught). This dislocation produces a double ascending jump in the flow. In extreme cases, the convective core passes out of the domain before any steady updraught structure is achieved. In marginal cases, a single updraught can sometimes be recovered after an initial episode with two ascent maxima. Inversely, it is also possible for a large meander to develop temporarily on a single updraught.

An example of a 'successful' development can be seen in Fig. 3. At the time shown ($t = 8\tau_m$), organization is essentially complete within a radius of $\Delta x = H$ from the gust front. The initial parameters for this case are $\eta_0 = 1.5\tau_m^{-1}$ and $h_0 = 0.3H$, with $b_c = -1.5b_m$. The frame of reference is that of the steady state, $M^* = -0.10V_mH$, which corresponds to $u_0 = -0.48V_m$ for the initial surface velocity. Three separate buoyancy maxima can be seen near the level $z = h_m$ (Fig. 3(b)). The central maximum is due to condensational heating, while the outer maxima are due to forced subsidence on the flanks of the updraught. The negative anomaly near the upper boundary indicates overshooting past the level of neutral buoyancy.

With its height of $0.3H$, the gravity-current 'head' is twice as high as the cooling region. The gravity current is just strong enough to create a weak rotor circulation at the ground, seen as a deflection of the zero stream-function contour in Fig. 3(a).

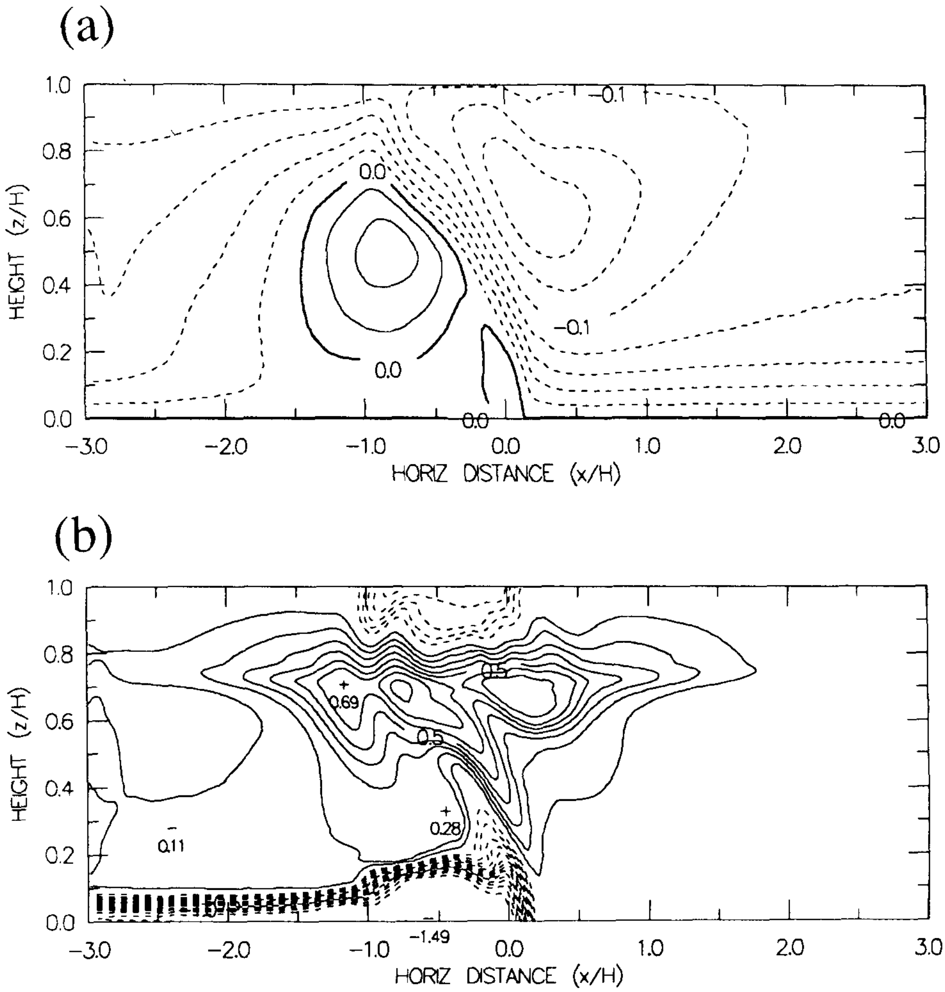

Figure 3. Plots of (a) total stream function, ψ, and (b) perturbation potential temperature, $b - \bar{b}$, at $t = 8\tau_m$ in first simulation. Contour intervals are $0.02V_mH$ (zero bold) and $0.1b_m$ (zero suppressed).

Otherwise, there is very little circulation in the cold pool. The downshear storm front, much broader than the gust front, is mostly confined to the interval $1 < x/H < 2$ at the time shown. The breadth of the storm front suggests that the signal is carried at least partly by linear waves (not necesarily gravity waves, since updraughts are assumed to be saturated in the layer $z_b < z < z_m$).

A case which fails to achieve a continuous, deep updraught is shown at the time $t = 8\tau_m$ in Fig. 4. The choices for η_0 and b_c are the same as in the first simulation, but the depth of the shear layer is reduced to $h_0 = 0.2H$ in the initial profile. The initial surface wind speed, $u_0 = -0.48V_m$, is the same as in the first case, which gives $M = -0.21V_mH$ (there is no critical value since the updraught does not become steady in a reasonable time). However, the wind at upper levels is $-0.15V_m$, compared with $-0.03V_m$ previously.

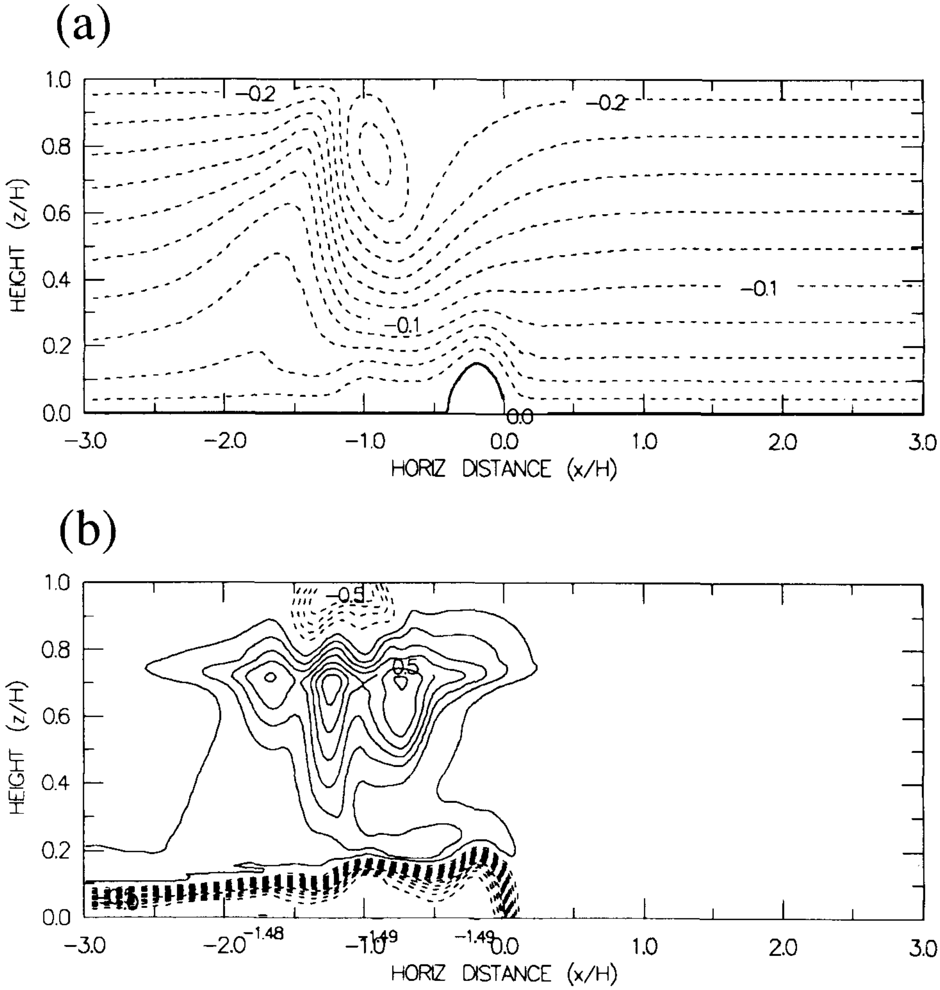

Figure 4. Plots of (a) total stream function, ψ, and (b) perturbation buoyancy, $b - \bar{b}$, at $t = 8\tau_m$ in second simulation. Compared with Fig. 3, there is a large horizontal displacement of the updraught from the gust front. Contour intervals as in Fig. 3.

At the time shown, the free updraught is still drifting away from the gust front, and will eventually reach $x = -2.5H$. The warm temperature anomaly (Fig. 4(b)) has the same qualitative features as in the first simulation, but is centred farther upshear and contracted horizontally. The narrowing is mostly a result of the diminished vertical mass flux in the meandering updraught. The upstream shift of the free convection places the compensating subsidence directly over the cold pool. This stands in contrast to the successful case, where the convective signal reaches the ground at a point downshear from the gust front. We shall return to this important contrast in section 4.

A summary of the full dependence on η_0 and h_0 is shown in Fig. 5. For a given pair of these parameters, the solution has been characterized as successful or unsuccessful according to whether the two updraughts reach their maximum separation during the first two hours ($\Delta t = 24\tau_m$). Reference to the cut-off time was necessary in only a few

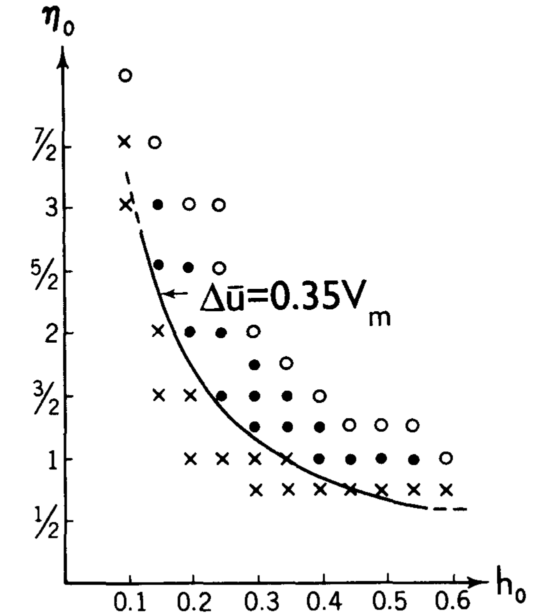

Figure 5. Classification of experiments as a function of low-level shear, η_0, and depth of shear layer, h_0. Points marked 'X' correspond to simulations that fail to achieve coherence between forced and free updraughts during first $\Delta t = 24\tau_m$. Cases marked with solid circles achieve updraught coherence within same period, but open circles indicate steady states with vertical or downshear-tilting updraughts. The relationship $\Delta\bar{u} \equiv \eta_0 h_0 = 0.35V_m$. is shown by the curve.

marginal cases since the majority of the successful simulations developed a single updraught within less than an hour. Using a cut-off time of $\Delta t = 36\tau_m$ produces only a small shift in the boundary between the two regimes. In this sense, the successful and unsuccessful cases are well differentiated.

In a less idealized context, a double jump is not necessarily a sign of short-lived convection. Even TMM's most vigorous squall line exhibits such a structure, and there is an obvious double jump in the California frontal line convection studied by Carbone (1982). Thus, the sustained single updraught in Fig. 3 should be viewed as a time-averaged structure, rather than as an instantaneous observation of realistic moist convection. We propose that the difference between squall lines and ordinary cumulonimbus lies essentially in the degree of coherence between the time-averaged positions of the forced and free updraughts. The failed simulation described above may be viewed as the model's representation of an ordinary cumulonimbus event. It also bears a resemblance to the decaying stage of the squall line simulated by RKW.

It is clear from the shape of the boundary between the regimes in Fig. 5 that neither the low-level vorticity nor the depth of the shear layer is by itself a good predictor of squall-line development. The most informative single parameter seems to be the *total* shear, $\Delta\bar{u} = \eta_0 h_0$. In the present circumstances, the boundary is well approximated by the curve $\Delta\bar{u} = 0.35V_m$ drawn in the figure. The figure also indicates that many of the cases on the successful side of the boundary are characterized by vertical or downshear-tilting updraughts. These would surely fail to produce sustained convection in a full-cloud model. Hence the truly successful cases fall within a narrow range of initial velocity difference $\Delta\bar{u}$. We consider next how the critical value, $(\Delta\bar{u})^*$, depends on characteristics of the cold pool and ambient stratification.

(b) *Sensitivity to cold-pool parameters and dry stratification*

For a relatively warm cold-pool with $b_c = -0.75b_m$, the development criterion is still found to depend essentially on the total shear, but with the boundary lowered to $(\Delta\bar{u})^* = 0.17V_m$, or roughly half the previous value. For the case of $b_c = -3.0b_m$, the boundary moves up to $(\Delta\bar{u})^* = 0.70V_m$, or double the original value. These variations of $(\Delta\bar{u})^*$ are in the same sense as the density-current velocity scale V_c, but are not proportional, since a doubling (halving) of b_c changes V_c by a factor of 1.4 (0.7). Nevertheless, the relationship between the critical shear and V_c is nearly linear. The best-fit relation

$$(\Delta\bar{u})^* = 1.6V_c - 0.33V_m \tag{4}$$

yields the three experimental values of critical $\Delta\bar{u}$ to within $0.02V_m$. The implication of Eq. (4) is that strong positive buoyancy makes it easier for the vertical shear to align the convective updraught with the gust front.

Extrapolation of Eq. (4) to the intercept $(\Delta\bar{u})^* = 0$ indicates that the shear will become altogether unnecessary when the convection is sufficiently strong ($V_m = 4.8V_c$). Indeed, it is possible to obtain steady states in the model when the convection is unrealistically strong (for example, $b_m = 5.0|b_c|$). As these solutions feature downshear tilts, they conflict with the assumptions behind the parametrized precipitation dynamics. Nevertheless, the decreasing importance of the shear seen in the experimental large-buoyancy limit points to a basic mechanism determining the phasing of the forced and free updraughts. In section 4, we look for a development scenario consistent with the results summarized by Eq. (4).

To emphasize the conclusion that the development depends on $\eta_0 h_0$ rather than on η_0 alone, we show a solution in Fig. 6 in which $\bar{\eta} = 0$ over the depth of the cooling region ($0 \le z \le 0.15H$), but $\Delta\bar{u} = 0.53V_m$ because of an elevated shear layer in $0.15H \le z \le 0.30H$. The cold-pool temperature is unchanged. It is evident from the figure that these conditions allow the development of a classic long-lived structure. Yet the elevation of the environmental shear layer eliminates any direct interaction between the ambient vorticity and that generated at the gust front. Superposition of ambient and perturbation circulations suggests no direct counteraction by the cold pool. Note that the total shear ($\Delta\bar{u} = 0.53V_m$) in this case would produce a downshear-tilting updraught if the shear layer were ground based, according to Fig. 5. Changing the profile shape alters the relationship of the total shear and surface stagnation pressure to the total mass and momentum fluxes. This apparently shifts the boundary between favourable and unfavourable environmental conditions in parameter 'space'.

Before examining the steady states in greater detail, we consider briefly how the development depends on cold-pool depth and ambient stratification. The scale V_c is directly proportional to the square root of h_c as well as $-b_c$. However, the cold-pool depth h_c further influences the flow by restricting the outflow depth to $H - h_c$. This additional constraint is well known from the classical analysis of Benjamin (1968) and the recent analytical model of Moncrieff and So (1989), although results of such models need not apply to the time-dependent problem. For values of h_c ranging from $0.10H$ to $0.30H$, we find that Eq. (4) continues to hold quite well. For the smaller values in this range, single updraughts tend to develop meanders (double jumps) more readily than for deeper cold pools with the same V_c. However, these developments do not affect the results summarized by Eq. (4).

Until now, a value of unity has been used for α, the ratio of the total dry stratification $\Delta\bar{b}$ below $z = h_m$ to the maximum lifted anomaly b_m. For much larger values of α, recirculation of air in the anvil raises the temperature there well above the theoretical

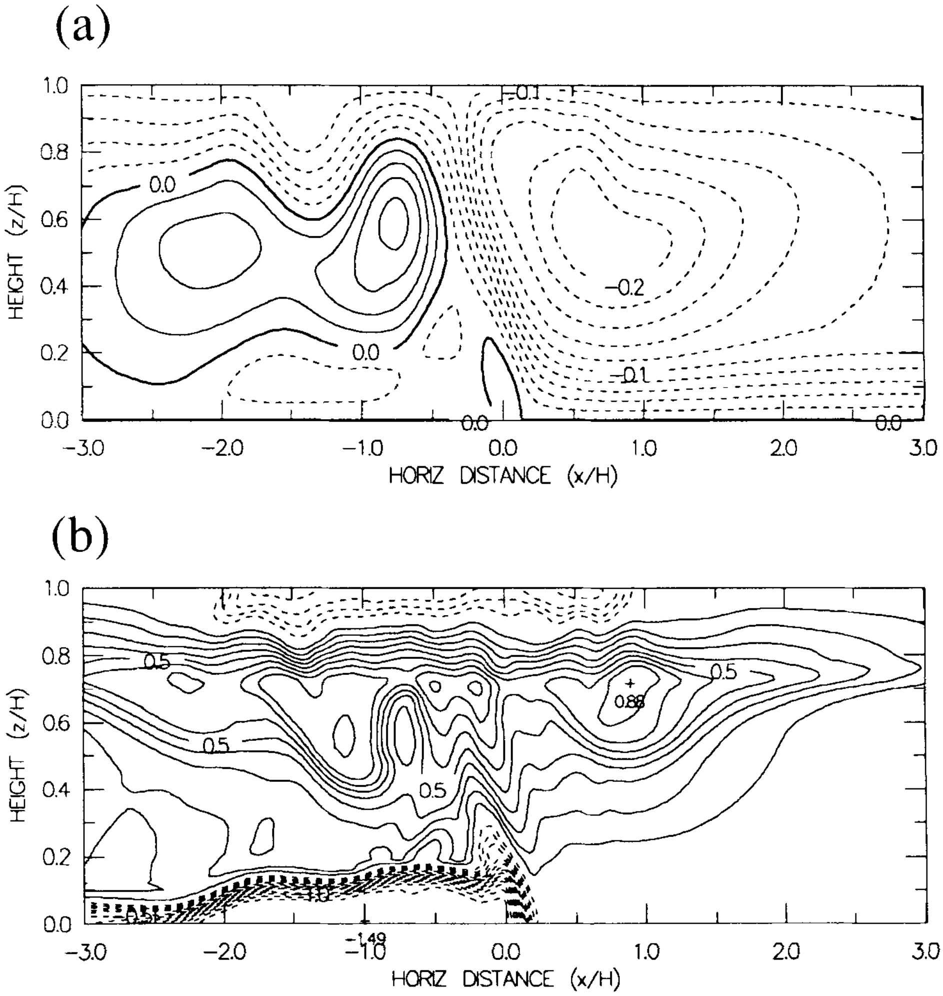

Figure 6. Plots of (a) total stream function, ψ, and (b) perturbation buoyancy, $b - \bar{b}$, at $t = 12\tau_m$ in simulation with elevated shear layer. Contour intervals as in Fig. 3.

bound b_m, as mentioned in section 2. However, since initial development may not be significantly affected by this model shortcoming, we have considered the case $\alpha = 3$, chiefly in order to test the sensitivity to the ambient wave-propagation speed. Despite the faster linear wave speed, no important differences are seen in the development process. In the long term, if the anvil temperature is capped at b_m, differences appear in: (1) a weaker overturning updraught on the forward side and (2) a broader jump updraught.*

(c) *Characteristics of the steady states*

The results on the initial conditions have no direct bearing on questions about steady-state maintenance such as Moncrieff and So (1989) and other analytical modellers have considered. Once the subsidence wave overtakes the gust front, and the overturning

* If the maximum-temperature anomaly is not controlled, the cold pool eventually surges away from the initial steady frame and the squall line collapses.

updraught is established on the downshear side, the environmental flow becomes irrelevant except for the shear and potential buoyancy of the surface layer. RKW have minimized the distinction between development and steady state because of the cell regeneration process. However, as noted in the introduction, there are components of a mature convective system that are clearly not dominated by the transience associated with individual cells. These include the disturbed far-field inflow and outflow profiles (and related vertical fluxes of momentum and heat) as well as the cold pool.

We look first at the far-field velocities on the upshear and downshear side of the gust front. The temperature and flow structure at $t = 48\tau_m$ in the first simulation are shown in Fig. 7. The flow at that time is essentially steady throughout the domain (only two-thirds of which is shown). The storm front, with its warm anvil and overlying cold anomaly, reaches the lateral boundaries at about $t = 32\tau_m$ in this case. Some of the thermal anomaly associated with the upper-level storm front remains in the picture at the time shown. Subsidence has stabilized the environment everywhere above cloud base. The edge of the cold air has settled slightly upwind of the edge of the cooling (always at $x = 0$). Since $\psi = 0$ along the lower boundary, the contour $\psi = M$ is the

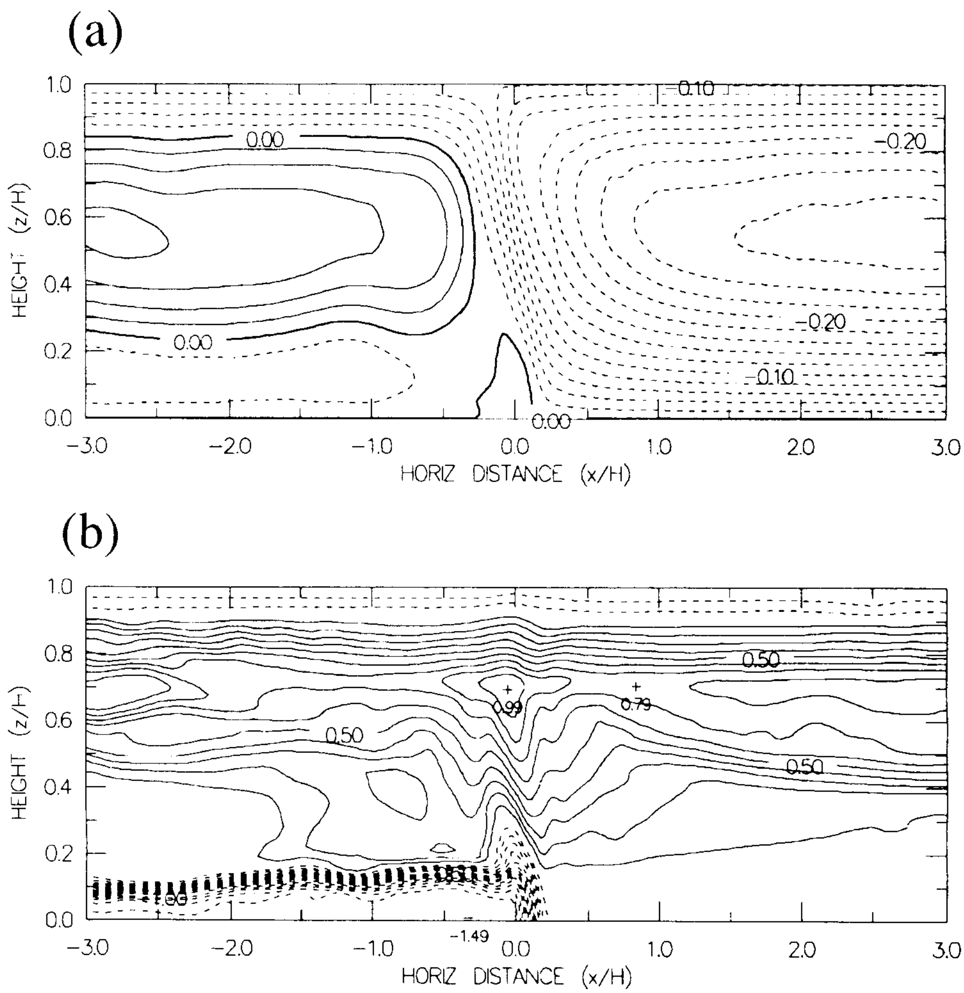

Figure 7. Plots of (a) total stream function, ψ, and (b) perturbation buoyancy, $b - \bar{b}$, in first simulation at $t = 48\tau_m$, showing quasi-steady state. Contour intervals as in Fig. 3.

interface between the jump and overturning updraughts in the steady state. The level of this streamline at the far right has dropped from the upper boundary to $z = 0.16H$ during the simulation.

The wind profiles in Fig. 8 are taken from the first simulation at time intervals of $12\tau_m$ along $x = \pm 2.0H$. The strong alteration of the profile over time confirms that the original environmental wind will not be relevant in a dynamical understanding of the two-dimensional quasi-steady system, as argued also by Lafore and Moncrieff (1990) from field observations. The surface wind speed at the right increases from $u = -0.48V_m$ to $u = -0.84V_m$. The forward overturning updraught, with its zero net mass flux, replaces the environmental flow above the level of $\psi = M$. A rear overturning updraught is evident in the other sequence of profiles in Fig. 8. The diverging outflows at the top of the model settle to speeds of about $\pm 0.7V_m$.

There is less shear in the front-to-rear outflow (Fig. 8(a)) than in the forward overturning outflow (Fig. 8(b)), probably because of an homogenization of the jump-updraught temperatures by mixing at the gust front. Some preliminary experimentation

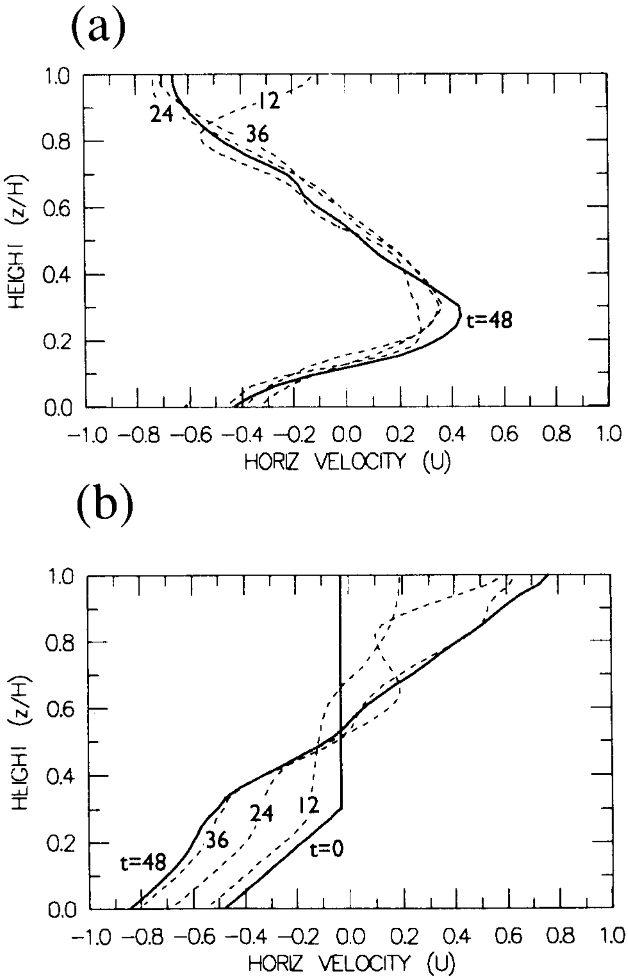

Figure 8. Profiles of far-field horizontal velocity at intervals of $12\tau_m$ measured at the (a) rear and (b) front of the squall line produced in the first simulation.

with thermal diffusivity has suggested to us that this mixing of heat is instrumental in allowing a jump updraught to remain laminar without ever overturning its (initially) unstable air supply. Strong negative vorticity is confined to the base of the jump outflow near $z = 0.85H$ and to the entire rear overturning updraught. The rear circulation is 'strong' according to the empirical classification by Smull and Houze (1987). A strong rear inflow jet occurs throughout the simulation by Fovell and Ogura (1988) but does not develop until the 'decaying' phase of that by RKW.

The increase in surface inflow wind speed implies a surface pressure drop between the model and the undisturbed environment of about 2 mb for typical parameter values. A similar drop was obtained recently in a three-dimensional cloud-model simulation by Lipps and Hemler (1991). These numerical results are quite consistent with the strength of the 'meso-low' observed by Hoxit *et al.* (1976) in advance of a line of cumulonimbus clouds in the mid-western USA. Their analysis shows that the amplitude of the surface low-pressure anomaly can be estimated from hydrostatic balance and an assumption of a relatively weak pressure disturbance above the subsidence warming. It is clear from the present simulations, as well, that vertical accelerations are negligible in the storm front.*

The incompressibility assumption tends to under-estimate the *depth* of the forward overturning outflow. However, the total mass flux displaced by the overturning updraught and the depth of its inflow layer are apparently not very sensitive to the vertical density gradient. An anelastic version of the present model produced a solution with only small differences in surface flow and overall development. Most three-dimensional cloud-model simulations (e.g. Lafore and Moncrieff 1989, Fovell and Ogura 1988) show a much smaller increase in the downshear surface inflow speed. Instead, the compensating front-to-rear flux tends to be concentrated at middle levels (the *total* front-to-rear mass-flux increase seems comparable with ours). The implicit decrease in low-level shear in the cloud-model simulations (see Lafore and Moncrieff 1990) may or may not be more realistic, but is precluded by our lateral and lower boundary conditions on vorticity and temperature.

One of the foundations of analytical models is the so-called flow-force principle (e.g. Benjamin 1968), which states that in a frame where the column-integrated horizontal momentum, M, is steady, the flow force, $F = \int (u^2 + p)\mathrm{d}z$, is the same on both sides of the storm (here we use p for the dynamic pressure). In Fig. 9 are shown profiles of $\Delta(u^2)$ and Δp, where Δ indicates the difference from the left to the right across the updraught. For convenience, the pressure is determined from an assumption of hydrostatic balance, with the lower-boundary value established from Bernoulli's principle.† The pressure difference integrates to about $0.9V_{\mathrm{m}}^2H$, whereas the momentum flux integrates to $1.1V_{\mathrm{m}}^2H$. The 20% discrepancy is due to momentum fluxes through the rigid boundaries and to inaccuracies in the (discretized) vorticity–stream-function treatment of momentum and pressure.

The flow-force evaluation suggests that analytical models can be useful for characterizing steady states in terms of the *disturbed* far-field profiles. The pressure profiles show that about two-thirds of the perturbation is associated with the surface stagnation

* Bernoulli's principle can be used to show that the pressure perturbations are about equal and opposite on the two boundaries in these solutions. However, an experiment using a raised upper boundary yielded substantially reduced upper-level velocity and pressure anomalies because of a deeper layer of cold anomaly above the level of neutral buoyancy.

† The model's explicit diffusion has been formulated with a condition of zero perturbation vorticity flux across boundaries and no heat flux. It can be shown that even in a diffusive steady flow, these conditions preserve the validity of Bernoulli's principle along a boundary. Application of the principle along the upper boundary in the model solution yields essentially the same values of Δp as shown in the figure.

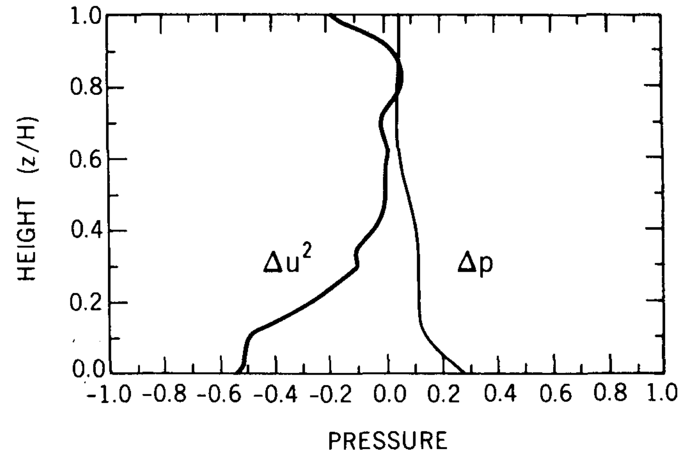

Figure 9. Profiles of horizontally integrated horizontal momentum flux divergence, $\Delta(u^2)$, and horizontal pressure gradient, Δp. In an inviscid model, the sum $\Delta(u^2+p)$ is the vertical convergence of momentum flux, $-\partial(uw)/\partial z$, integrated across the storm.

point, and the remainder with the difference in outflow velocities in the overturning and jump updraughts. There is little contribution to Δp from the positive buoyancy anomalies, since they are distributed more or less symmetrically around the updraught. The momentum budget contains information about the updraught tilt in the form of the correlation between u and w. The solutions with vertical or downshear tilts, marked by open circles in Fig. 5, are characterized by relatively small values of horizontal momentum flux. As noted in the introduction, the neglect of superposed transience in these conclusions finds justification in the numerical study by Fovell and Ogura (1988).

4. Discussion

The results of section 3 suggest a criterion for squall-line development that is different from previously emphasized factors such as updraught tilt. It appears that the environment must allow the initial 'thermal' to reach its level of neutral buoyancy while it is still close enough to the gust front to avoid placing subsidence over the cold pool. Figure 10 shows that there are already crucial differences between the successful and unsuccessful simulations by $t = 4\tau_m$. The results are from the first two simulations of section 3, both of which have $\eta_0 = 1.5\tau_m^{-1}$ for the initial low-level shear. The latent heating has increased the vorticity by a factor of 2 or 3. Subsidence occurs to the right of the positive-vorticity anomalies. Significantly, it is concentrated over the gust front in the unsuccessful case, but downshear from the cold air in the successful simulation (the edge of the cold air is not marked, but coincides approximately with the zero vorticity contour).

When subsidence takes place to the rear of the gust front, the storm-front pressure drop mentioned in section 2 occurs over the cold air and draws the air forced up at the gust front laterally into the convective updraught. This not only allows the separation between the two updraughts to continue widening but also permits mid-level air to enter the convection and reduce the buoyancy. By contrast, if conditions are such that the storm front can move rapidly ahead of the gust front, the head of the density current can adjust to the stronger surface flow by becoming deeper or drifting upshear in the direction of the free convection. In this subcritical case, air entering the convective updraught has more potential buoyancy and less lateral momentum relative to the gust front.

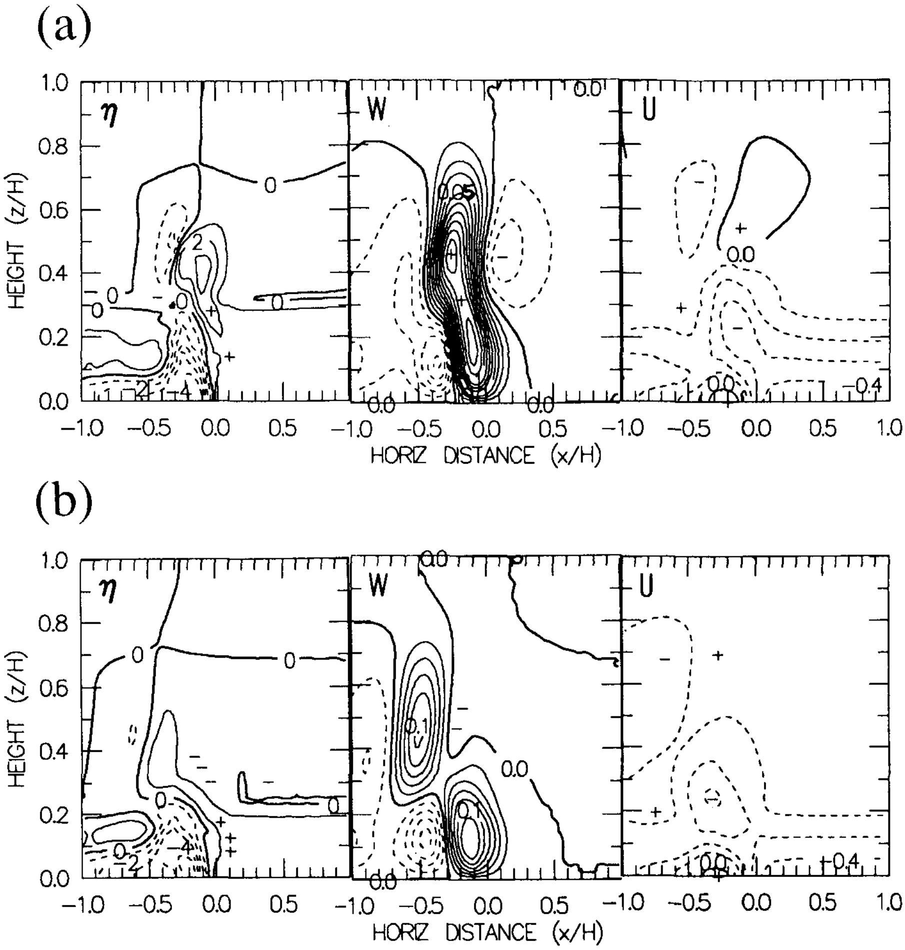

Figure 10. Total horizontal vorticity, η, and components u and w of total velocity at $t = 4\tau_m$ in (a) first and (b) second simulations. Of interest is the location of the subsidence ($w < 0$) relative to the gust front in the respective cases (for practical purposes the gust front coincides with the $\eta = 0$ contour near the ground). Contour intervals: $\Delta\eta = 1.0\tau_m^{-1}$, $\Delta w = 0.05V_m$ and $\Delta u = 0.1V_m$.

The positive feedback on the updraught separation in unsuccessful cases and the negative feedback in successful cases appear to account for the sharpness of the parameter regime boundary found in section 3. A closely related feedback between convective heating and low-level convergence was invoked by Raymond (1983) to account for the growth and propagation of wave-CISK modes. As we have seen, the present subsidence signal contains an additional nonlinear component in the form of a relatively slow-moving inverted gravity current at the neutral buoyancy level. The feedback on the gust-front convergence may also depend on details of the rear overturning updraught. With or without these complications, the organization of a surface updraught by an elevated heat source represents a separate mechanism from the kind of local organization hypothesized by RKW.

Tests mentioned in section 3 showed a lack of sensitivity of the early development to the ambient dry stratification. In this sense, the downward signal propagation from the initial heating must be fast even for the weakly stratified atmosphere used in the long-term experiments. A more important factor determining the location of the initial subsidence is probably the lateral speed of the free updraught relative to the gust front.

In a two-layer atmosphere with no boundaries, growing modes of dry convection travel at the average speed of the layers, as in the (gravitationally stable) Kelvin–Helmholtz problem. Studies with continuous shear by Kuo (1963) and Bolton (1984) also show normal modes tending to move with the average velocity of the basic wind. If an upper boundary is introduced, a separate 'gravitational' mode becomes possible, and moves at essentially the speed of the upper layer (Orlanski and Ross 1986).

If the principles behind these results are applicable to the initial-value problem (despite the up–down asymmetry of moist convection), they explain the tendency for the free updraught in the squall-line simulations to move away from the gust front more rapidly at first if there is a stronger upper-level relative wind. A dimensional approach can now be followed to obtain a formula for the critical shear. We may first assume that the free updraught moves at the speed $u_1 + \beta\Delta u$, where u_1 is the wind speed at the top of the cold pool (in the frame of the gust front) and β depends on how heavily the upper-level flow should be weighted in the average. For example, if the ascent maximum moves with the simple average of the lower and upper speeds, and if vorticity is conserved, then $\beta = \frac{1}{2}$.

The time required for the thermal to reach neutral buoyancy and for the subsidence to develop can be expressed as $\Delta t = r\tau_m$, where r is non-dimensional and O(1). If we assume that $u_1 = -kV_c$, with $k = O(1)$, the separation of the updraughts after an elapsed time of Δt is:

$$\Delta x = (kV_c - \beta\Delta u)rH/V_m.$$

The value of Δx that makes organization marginally possible should depend on how far the subsidence wave can move downshear, and on how wide the updraught becomes during the time Δt. If the width is determined by non-hydrostatic effects, it is commensurate with H (though some dependence on the depth of the shear layer is also possible). The linear signal displacement would also scale with H (and $\alpha^{1/2}$), but it is not expected to be as important, in view of the sensitivity tests mentioned earlier.

Thus, the critical value of the displacement is $(\Delta x)^* = \varepsilon H$, with $\varepsilon = O(1)$. With this substitution, we have that

$$(\Delta u)^* = aV_c - bV_m \tag{5}$$

where $a = k/\beta$ and $b = \varepsilon/r$. If the cold-air depth is much less than H, then u_1 is essentially the same as the disturbed surface flow at the far right (and k is approximately the gravity-current Froude number). With $\beta = \frac{1}{2}$, the empirical choice $k \approx 1$ (Benjamin 1968) gives $a \approx 2$. Since τ_m is an e-folding time for the changes in altitude of a buoyant parcel (say from $0.2H$ to $0.9H$), $r \approx 2$ is reasonable, and we get $b \approx 0.5$ when $\varepsilon = 1$. These estimates for a and b are in good agreement with the experimental values 1.6 and 0.33 appearing in Eq. (4).

In RKW's analysis, the scale V_c is introduced by assuming surface flow stagnation and zero pressure anomaly above the cold pool. These are necessary conditions for a steady vertical updraught. In the above development, the scale V_c enters in a more conventional way through an assumption of flow stagnation and overall mass conservation. In conjunction with flow stagnation, mass conservation in flow over a shallow obstacle has nearly the same quantitative implications as zero pressure perturbation over the obstacle (i.e. $k \approx 1$). Hence, the more consequential difference between the two theories is the appearance in Eq. (5) of the CAPE scale V_m. This is the term that brings in the aforementioned distant feedback mechanism. Free convection is considered passive in RKW's theory, which therefore cannot account for any dependence of the criticality on the convective potential energy.

A special set of time-dependent simulations by RKW show that the vertical penetration of a forced updraught can be maximized by adjusting the ambient shear.* How important this result is probably depends mostly on the convective stability (negative area) in the thermodynamic sounding. Since we have suppressed cell decay and redevelopment to concentrate on the larger circulation, it is beyond our scope to investigate the effect of different amounts of negative area. In the experiments with zero negative area, it was found that the tilt of the forced updraught has little to do with the tilt or movement of the convective plume (once triggered) and is therefore not strongly related to the *total* updraught tilt. This result was established independently by Lafore and Moncrieff (1990) from their tropical squall-line data. It is also clear, from the full set of experiments, that changing the low-level vorticity does not make the free updraught any more or less erect.

To appreciate the independence of the total updraught tilt, consider the close-up view of the disturbance at $t = 4\tau$ (Fig. 10). There are no important differences in the tilt of the forced updraught between the first and second simulations (which had identical low-level shear), even though dramatic differences appear in the subsequent storm development. The updraughts are weaker in the unsuccessful case, but we attribute this to their unfavourable phase relationship and to the entrainment of mid-level air into the convective updraught. Hence, we conclude, with Lafore and Moncrieff (1990), that low-level vorticity dynamics are, at most, secondary in importance to the larger circulations in modulating squall-line intensity.

One of the weaknesses of the present theory is the modelling assumption that all levels of the atmosphere up to $z = h_{\mathrm{m}}$ are equally unstable to small vertical displacements. This makes the kinetic energy of the initial thermal greater than it might be in soundings with more stable middle tropospheres. We have already commented on the relative ease with which the model achieves single updraughts in cases where more sophisticated models might generate double jumps instead. We believe that the strong conditional instability at middle levels contributes to this bias without invalidating the distinction between successful and unsuccessful cases based on the degree of coherence between the forced and free updraughts.

The time of Fig. 10 is close to that when more realistic convection begins to collapse or divide under the burden of negative buoyancy in the updraught. Thus, the suppression of new convection near the gust front by the old convection may be artifically strong in the second simulation (cf. Fig. 4). The model compensates for this in two ways: by omitting any negative area in the thermodynamic sounding, and by maintaining the cold pool even as the updraught moves away. Since negative area and cold-pool dissipation would also suppress new cells, we hold to our belief that the unsuccessful simulation is an accurate depiction of a terminal process in the life of the convection. If new cells cannot develop until the circulation from the old cells has died away, the cold pool and surface convergence may be too weak to sustain the mesoscale organization. Certainly, our 'failed' simulation resembles the decaying phase of RKW's storm, although we cannot be sure that the suppression in their solution is due principally to the convective downdraught (instead of the negative area).

5. Summary and conclusion

By producing extraordinarily steady long-term solutions, the simplified model brings the squall-line organizational process into high relief. Examination of the long-term

* By contrast, their *analytical* condition involving V_{c} applies to the *total* shear Δu and does not actually determine the updraught orientation.

solutions suggests that classical models like those of Benjamin (1968) and Moncrieff (1978) can be relied upon for understanding aspects of the quasi-steady dynamics. Unfortunately, results from the steady-state models cannot shed much light on the dynamical constraints that distinguish squall lines from the more common variety of moist convection.

The more relevant initial-value problem of linearized convection in shear is relatively intractable (judging from the lack of classical analytical results). However, some useful insight may be available from the no-shear problem. Raymond (1983) solved that problem as part of an effort to understand normal-mode wave-CISK. His discussion about the propagation of the surface convergence maxima is reminiscent of our theory in section 4 for how convective heating initially organizes or disorganizes the updraught. We have tried to include the shear in this mechanism by referring to normal-mode solutions of convection in sheared environments. That line of thinking together with a dimensional analysis has led to a reasonably successful prediction of the minimum vertical contrast in line-normal environmental wind necessary for organization.

Rotunno *et al.* (1988) have made a fundamental contribution in directing attention to the squall-line development process. However, the theory of vorticity matching neglects changes in ambient conditions due to the establishment of a forward overturning updraught and other permanent features, as pointed out by Lafore and Moncrieff (1990). A similar criticism applies to the traditional conceptual view (TMM) of the role of the ambient shear because of the assumed continuous transfer of momentum from the undisturbed environment to the free updraught. The necessity of optimal forced updraughts in the cell regeneration process probably depends on the convective inhibition in the environmental sounding. Although we have not investigated this dependence, we doubt that low-level vorticity dynamics based on ambient conditions can have much to do with convective intensity after the squall line is organized.

We have argued that the development phase of organized convection may have a nearly linear explanation. By contrast, the long-lived states that arise from favourable initial conditions are quite nonlinear. The mature updraught consists mainly of air originating from the surface, rather than middle and upper levels, and most of the low-level air never enters the surface cold region as in a linear model. Nonlinear analytical models like those of Green and Pearce (1962), Moncrieff (1978) and Moncrieff and So (1989) are more relevant for the long-term circulation. These have already served to demonstrate that a range of steady states become possible with the inclusion of energy dissipation or overturning updraughts and downdraughts. An important target for future research is the principle by which a particular one of these states is selected.

Our speculation on the last question is that the selection may have to do with the variation during start-up of *internal* parameters such as cold-pool height, rear-inflow jet speed and, especially, net lateral mass flux measured in the frame moving with the gust front. A successful nonlinear development may be seen as a crossing, in parameter space, into a region where steady structures are possible. Thus, an important question for future work is whether the boundary between existence and non-existence of steady states in the most comprehensive analytical model has strong dependence on one or more of the internal parameters.

ACKNOWLEDGEMENTS

Discussions with Dr Richard Rotunno and Dr Frank Lipps are gratefully acknowledged. We thank Dr Bryan Johns and Dr Ming Xue for acquainting us with the advection schemes and Prof. Brian Hoskins for sharing his opinions about the direction of the research. We are also grateful for the careful reviews provided by Dr Mitch Moncrieff and Dr Robert Fovell. The first author received support from the Meteorological Office and through the AOS Program at Princeton University (USA).

Appendix

List of symbols

b	potential buoyancy, $g\theta/\theta_0$, where θ is the potential temperature and θ_0 a reference value
b_m	maximum lifted buoyancy relative to initial profile
b_c	potential buoyancy of cold pool (mid-level wet-bulb potential temperature)
g	acceleration of gravity
h_b	depth of well-mixed surface layer
h_c	depth of cooling region
h_m	level of maximum lifted potential temperature
h_t	level of neutral buoyancy for lifted surface parcels
l_c	width of cooling region
p	pressure divided by density
u	horizontal velocity component
w	vertical velocity component
x	horizontal coordinate
z	vertical coordinate
H	height of domain
M	total horizontal mass flux, $\int u dz$
V_c	gravity-current velocity scale, $\surd(-b_c H)$
V_m	convective velocity scale, $\surd(b_m H)$
γ	rate of change of potential temperature with height of lifted parcel
η	horizontal vorticity, $\partial u/\partial z - \partial w/\partial x$
τ_c	time scale of non-adiabatic cooling
τ_m	convective time scale, $\surd(H/b_m)$
ψ	stream function for flow in vertical section
$\overline{(\ )}$	denotes initial value
$(\ )^*$	denotes critical value

References

Benjamin, T. B. 1968 Gravity currents and related phenomena. *J. Fluid Mech.*, **31**, 209–248

Betts, A. K. 1976 The thermodynamic transformation of the tropical subcloud layer by precipitation and downdrafts. *J. Atmos. Sci.*, **33**, 1008–1018

Bluestein, H. B. and Jain, M H. 1985 Formation of mesoscale lines of precipitation: severe squall lines in Oklahoma during the spring. *J. Atmos. Sci.*, **42**, 1711–1732

Bolton, D. 1984 Generation and propagation of African squall lines. *Q. J. R. Meteorol. Soc.*, **110**, 695–721

Browning, K. A. and Ludlum, F. H. 1962 Airflow in convective storms. *Q. J. R. Meteorol. Soc.*, **88**, 117–135

Carbone, R. E. 1982 A severe frontal rainband. Part I: stormwide hydrodynamic structure. *J. Atmos. Sci.*, **39**, 258–279

Dudhia, J., Moncrieff, M. W. and So, D. W. K. 1987 The two-dimensional dynamics of West African squall lines. *Q. J. R. Meteorol. Soc.*, **113**, 121–146

Emanuel, K. A. 1986 Some dynamical aspects of precipitating convection. *J. Atmos. Sci.*, **43**, 2183–2198

Fovell, R. G. and Ogura, Y. 1988 Numerical simulation of a midlatitude squall line in two dimensions. *J. Atmos. Sci.*, **45**, 3846–3879

Green, J. S. A. and Pearce, R. P. 1962 'Cumulonimbus convection in shear'. Imperial College, Dept. of Meteorology, Technical Note 12

Hoxit, L. R., Chappell, C. F and Fritsch, J. M. 1976 Formation of mesolows or pressure troughs in advance of cumulonimbus clouds. *Mon. Weather Rev.*, **104**, 1419–1428

Kuo, H. L. 1963 Perturbations of plane Couette flow in stratified fluid and origin of cloud streets. *Phys. Fluids*, **6**, 195–211

Lafore, J.-P. and Moncrieff, M. W. 1989 A numerical investigation of the organization and interaction of the convective and stratiform regions of tropical squall lines. *J. Atmos. Sci.*, **46**, 521–544

1990 Reply to Rotunno *et al.* (1990). *J. Atmos. Sci.*, **47**, 1034–1035

Lilly, D. K. 1979 The dynamical structure and evolution of thunderstorms and squall lines. *Ann. Rev. Earth Planet. Sci.*, **7**, 117–171

Lipps, F. B. and Hemler, R. S. 1991 Numerical modeling of a midlatitude squall line: features of the convection and vertical momentum flux. *J. Atmos. Sci.*, **48**, 1909–1929

Meischner, P. F., Bringi, V. N., Heimann, D. and Holler, H. 1991 A squall line in southern Germany: kinematics and precipitation formation as deduced by advanced polarimetric and Doppler radar measurements. *Mon. Weather Rev.*, **115**, 678–701

Moncrieff, M. W. 1978 The dynamical structure of two-dimensional steady convection in constant vertical shear. *Q. J. R. Meteorol. Soc.*, **104**, 563–567

1981 A theory of organized steady convection and its transport properties. *Q. J. R. Meteorol. Soc.*, **107**, 29–50

Moncrieff, M. W. and Miller, M. J. 1976 The dynamics and simulation of tropical cumulonimbus and squall lines. *Q. J. R. Meteorol. Soc.*, **102**, 373–394

Moncrieff, M. W. and So, D. W. K. 1989 A hydrodynamical theory of conservative bounded density currents. *J. Fluid Mech.*, **198**, 177–197

Ogura, Y. and Liou, M.-T. 1980 The structure of a midlatitude squall line: a case study. *J. Atmos. Sci.*, **37**, 553–567

Orlanski, I. 1976 A simple boundary condition for unbounded hyperbolic flows. *J. Comput. Phys.*, **21**, 251–269

Orlanski, I. and Ross, B. B. 1986 Low-level updrafts in stable layers forced by convection. *J. Atmos. Sci.*, **43**, 997–1005

Raymond, D. J. 1983 Wave-CISK in mass flux form. *J. Atmos. Sci.*, **40**, 2561–2572

Redelsperger, J.-L. and Lafore, J.-P. 1988 A three-dimensional simulation of a tropical squall line: convective organization and thermodynamic vertical transport. *J. Atmos. Sci.*, **45**, 1334–1356

Rotunno, R., Klemp, J. B. and Weisman, M. L. 1988 A theory for strong, long-lived squall lines. *J. Atmos. Sci.*, **45**, 463–485

1990 Comments on 'A numerical investigation of the organization and interaction of the convective and stratiform regions of tropical squall lines'. *J. Atmos. Sci.*, **47**, 1031–1033

Smull, B. F. and Houze, Jr., R. A. 1985 A midlatitude squall line with a trailing region of stratiform rain: radar and satellite observations. *Mon. Weather Rev.*, **113**, 117–133

1987 Rear inflow in squall lines with stratiform precipitation. *Mon. Weather Rev.*, **115**, 2869–2889

Thorpe, A. J., Miller, M. J. and Moncrieff, M. W. 1982 Two-dimensional convection in nonconstant shear: A model of mid-latitude squall lines. *Q. J. R. Meteorol. Soc.*, **108**, 739–762

Zalesak, S. T. 1979 Fully multi-dimensional flux-corrected transport algorithms for fluids. *J. Comput. Phys.*, **31**, 335–362